

Synthesis of 5,6-Spiroethers and Evaluation of their Affinities for the Bacterial A Site

Ioannis A. Katsoulis, Georgia Kythreoti, Athanasios Papakyriakou, Konstantina Koltsida, Panoula Anastasopoulou, Christos I. Stathakis, Ioannis Mavridis, Thomas Cottin, Emmanuel Saridakis, and Dionisios Vourloumis*^[a]

Natural aminoglycoside antibiotics and their corresponding chemical analogues are superb molecular tools for the exploration of the subtle interactions that underlie the biological regulation of RNA sequences.^[1] One prominent example is to be found in molecules that target the bacterial ribosomal RNA, cause the disruption of protein synthesis and by this validated mechanism exert their pharmacological activity.^[2] Understanding of the structural elements that lead to molecular recognition of RNA is constantly improving with the identification of aromatic interactions^[3]—alongside the known electrostatic ones^[4]—that enable high-affinity binding. Moreover, it has been theorized that the conformational versatility of the implicated chemical entities plays an important role for specific binding to the desired RNA site.^[5] Despite the challenges that still confront the discovery and pharmacological application of new aminoglycoside conjugates, the potential of such chemical entities to interfere with diverse biological processes remains highly attractive.^[6]

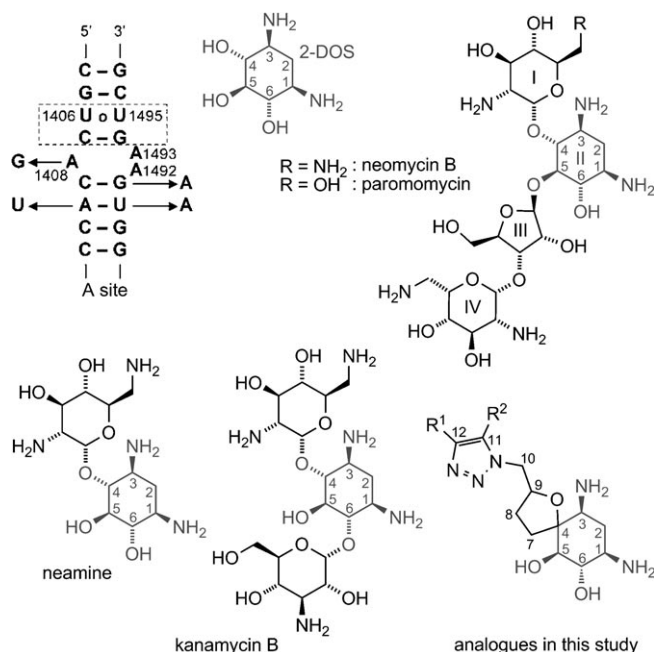
Our past endeavours in this field have focused on the synthesis and biological evaluation of rigid spirocyclic ethers^[7,8] that appear to capture the “bioactive” conformation within the A site of the ribosomal RNA (Scheme 1). In order to explore the chemical space that can be accessed by these means further, cyclic 5,6-spiroethers bearing triazole moieties were readily synthesized and assessed for their binding potentials. The choice of the triazole unit was predominantly governed by its ease of preparation, either by Cu-catalysed “click chemistry”^[9] or by thermal 1,3-dipolar cycloaddition.^[10] Moreover, triazoles have unique biological potential, possibly arising from π stacking with other aromatic^[11] or carbohydrate moieties^[3] of the RNA target, and therefore comprise an important pharmacophore for potential drug discovery.^[12] A noteworthy difference from past synthetic analogues of the same chemical family^[7,8] is the substitution pattern of the spiroether. The presented compounds are extended in their “northwestern” flanks with a set of functionalities that can satisfy and complement the condition of “structural electrostatic complementarity”^[4] within the active site.

[a] Dr. I. A. Katsoulis, Dr. G. Kythreoti, Dr. A. Papakyriakou, K. Koltsida, P. Anastasopoulou, Dr. C. I. Stathakis, I. Mavridis, Dr. T. Cottin, E. Saridakis, Dr. D. Vourloumis

Laboratory of Chemical Biology of Natural Products and Designed Molecules, Institute of Physical Chemistry N.C.S.R “Demokritos”, Agia Paraskevi–Athens, 15310 (Greece)
Fax: (+30)210-651-1776

E-mail: vourloumis@chem.demokritos.gr

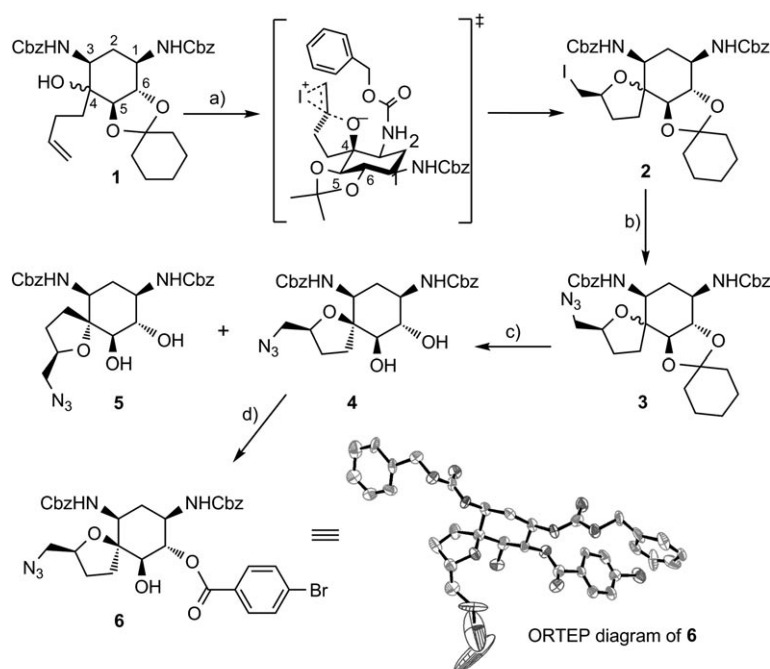
Supporting information for this article is available on the WWW under <http://dx.doi.org/10.1002/cbic.201100076>.



Scheme 1. Secondary structure of the bacterial decoding-site internal loop (A-site) in 16S rRNA. The four base changes in the eukaryotic sequence are indicated by arrows. The recognition site for the 2-DOS moiety of aminoglycosides is boxed. The structures of neomycin B, paromomycin, neamine (neomycin A) and kanamycin B all contain the 2-DOS core. Below right: general structure of the analogues described in this work.

The preparation of the spiroether moiety began with the common intermediate **1** (Scheme 2, 7:1 mixture of diastereomers at C4), previously utilized in our synthetic 6,7-membered series.^[7] On iodoetherification with *N*-iodosuccinimide^[13] this furnished the primary iodide **2**. This reaction appears to proceed stereoselectively, with regard to C9 (numbering presented in Scheme 1), as revealed in the ensuing steps (vide infra), with a possible transition state as depicted in Scheme 2. The observed selectivity could result from the minimization of steric interactions between the N3-Cbz and the electrophilic iodine.^[14] The iodide **2** was next converted into its corresponding azide **3**.^[15] Upon removal of the masking ketal, we were able to separate the two diastereoisomeric (at C4) 1,2-diols **4** and **5** (7:1 d.r.) by column chromatography. In order to verify the absolute configuration of the major isomer, **4** was converted to the monobenzoate ester **6** and X-ray crystallographic analysis provided decisive evidence for all its stereocenters (Scheme 2).

Our synthetic efforts continued with both isomers, producing a set of 12 new triazoles (**7–18**, Table 1), either by the standard “click-chemistry” procedure^[9] or through thermal 1,3-di-



Scheme 2. Reagents and conditions: a) NIS (1.0 equiv), NaHCO₃ (2.0 equiv), MeCN, 3 h, 0 → 25 °C, 78% yield; b) NaN₃ (3.5 equiv), DMF, 28 h, 50 °C, 89% yield; c) AcOH/THF/H₂O (3:3:1, v/v/v), 48 °C, 12 h, 79% for **4** and 11% for **5**; d) 4-bromobenzoyl chloride (3.0 equiv), TEA (4.5 equiv), DMAP (0.2 equiv), CH₂Cl₂ (0.05 M), 87%. NIS = *N*-iodosuccinimide; DMF = *N,N*-dimethylformamide; AcOH = acetic acid; THF = tetrahydrofuran; TEA = triethylamine; DMAP = 4-(dimethylamino)pyridine.

polar cycloaddition.^[10] The selection of the reactant alkynes was based on their sizes and on the nature and number of their functional groups, with the goal of identifying major interaction with the pertinent RNA sites. Specifically, the distance between the H-bond donor and the triazole (**9** vs **13**), the importance of dipolar as opposed to aromatic interactions (**11** vs **13**) and the natures (amine, amide, ether or hydroxy) and numbers of polar groups present (**10**, **13**, **15**–**17**), as well as the overall sizes of the small molecules (**13**, **15**, **16**, **18**), could thus be evaluated.

The affinities of all the spiroether triazoles towards the RNA A site were evaluated by RNA fluorescence assay (Table 1).^[16] A model RNA oligonucleotide in which the adenine at position 1492 had been replaced by a fluorescent probe (2-aminopurine, 2AP) was employed.^[16] The binding of the minor isomers **7** and **8** to the RNA construct proved to be relatively weak (low-μM concentrations, Table 1) in relation to that of the compounds resulting from functionalization of the isomeric azide **4**. Analogously to the reported six- and seven-membered analogues,^[7] the presence of the *S* configuration around the C4 quaternary centre is accompanied by improved affinity in most of the cases studied. Generally, the sizes of the triazole substituents appear to be the determining factor for potency, irrespective of the hydrogen-bonding potential present in the monosubstituted series (**13** vs **9**, **9** vs **15** and **17**, Table 1). Bulkier substituents (compounds **16** and **18**) resulted in complete inactivity. The analogue **11**, however, represents an exception to that observation, presumably because the expected unfavourable steric load could be compensated by favourable aro-

matic interactions. Of the mono-substituted analogues, the alcohol **13** represents the strongest binder, with affinity in the low-nM concentrations. This significant improvement relative to previously reported rigid spiroether analogues^[7,8] motivated a computational modelling attempt to interpret their atomic-level interactions with the A-site.

Docking of compounds **7**–**18** into a model of the rRNA A-site was performed as described previously.^[7,8] The calculated conformations of the most potent compound **13** exhibit a high degree of invariability with respect to its orientation within the A-site. This was also evident for all spiroether triazole compounds, because their docking to the decoding centre predicted at least four major clusters of putative orientations. Lack of any cocrystallographic data on these analogues bound to RNA makes our choice quite specula-

tive. However, two of the highest-affinity conformations calculated for compound **13** were found to overlap with the position of neamine in the corresponding cocrystal structure (see the Supporting Information). In the first one (Figure 1A), the aminocyclitol of **13** is proximal to ring II (2-DOS) of neamine, such that the triazole ring protrudes towards the two extruded A1492 and A1493 bases, stabilizing their conformation through a direct hydrogen bond between the hydroxy constituent and N7 of A1493. The aminocyclitol group provides the conserved hydrogen-bonding functionality of 2-DOS with the C1407–G1494 and U1406–U1495 base pairs. In the second “inverted” orientation, the aminocyclitol moiety is predicted to superimpose with ring I of neamine (Scheme 1) such that the triazole extends up to U1495 where it interacts with the phosphate backbone of G1494 (Figure 1B). The observed affinities of the spiroether triazole analogues could therefore potentially be explained by either binding mode.

In conclusion, we have successfully synthesized and evaluated small rigid molecular scaffolds that produce very good EC₅₀ values for the ribosomal A-site construct utilized in our fluorescent studies. These adducts avoid the excessive electrostatic charge of the natural products, which is a cause of adverse side effects for this class of compounds.^[18] The exact binding mode (orientation and site) of the spiroether triazole analogues is uncertain, and further biophysical biological^[19] and crystallographic efforts for this purpose are currently underway. Nevertheless, we expect them to contribute significantly to understanding of the principles governing RNA recognition and more specifically the dynamic interplay of the small-molecule

Table 1. The twelve triazoles **7–18** and their affinities towards the A site.

Alkyne	Conditions	Product	Alkyne	Conditions	Product / RNA affinity	RNA EC ₅₀
			conditions			
	[a], [b]			[d], [b]		950.2 mM (±46.6)
	[a], [b]			[a], [c]		452.8 mM (±10.9)
	[a], [b]			[d], [b]		22.2 nM (±5.4)
	[a], [b]			[d], [b]		43.2 nM (±0.6)
	[a], [b], [c]			[a], [b]		nonspecific binding
	[a], [b], [c]			[a], [b]		nonspecific binding
		neomycin			neamine	9.5 mM (±1.2)

[a] Alkyne, CuSO₄·5H₂O (0.3 equiv), sodium ascorbate (1.1 equiv), EtOH/H₂O (2:1), 25 °C. [b] Aq KOH (1.5 w), 125 °C. [c] Aq HCl (0.1 m), 40 °C. [d] Alkyne, toluene/MeOH (4:1), 140 °C, 20 h. [e] Low efficacy in fluorescence intensity effect.

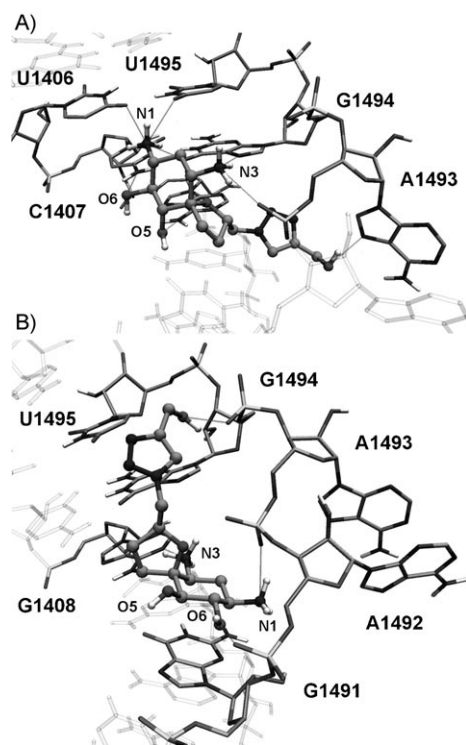


Figure 1. Predicted binding modes of compound **13** in the ribosomal A-site. A) Binding orientation of **13** with 2-DOS occupying the usual site of the aminoglycoside ring II, and B) alternative orientation with 2-DOS in the position corresponding to the aminoglycoside ring I (stacked over G1491). Intermolecular hydrogen bonding interactions are shown with red lines, carbon atoms in RNA are coloured orange, those in compound **13** in cyan, whereas all oxygen atoms are red, nitrogen blue and phosphorus yellow. Images were prepared with VMD 1.8.6^[17]

attributes with the adaptable structural and energetic landscape of the ribosomal A-site.^[20]

Experimental Section

Iodoetherification and azidation: The homoallylic alcohol **1** (0.26 g, 0.47 mmol) was dissolved in dry acetonitrile (4.0 mL) at 0 °C, and NaHCO₃ (78 mg, 0.93 mmol) and *N*-iodosuccinimide (0.11 g, 0.47 mmol) were added successively. The suspension was allowed to stir in the dark for 3 h and brine (5 mL) was added. The mixture was extracted with AcOEt (3 × 15 mL), dried (MgSO₄) and concentrated in vacuo. The solid crude product was purified by flash column chromatography on silica gel (prewashed with Et₃N) with a hexanes to hexanes/AcOEt (1:2) gradient elution system in order to afford the iodide **2** in the form of a white amorphous solid. (0.26 g, 78% yield). Sodium azide (71 mg, 1.087 mmol) was added at 50 °C to a solution of the iodide **2** (250 mg, 0.362 mmol) in dry DMF (4 mL). The reaction mixture was allowed to stir for 36 h, the solvent was then removed in vacuo, and the crude product was purified by flash column chromatography on silica gel, with a hexanes to hexanes/AcOEt (1:1) gradient elution system, to afford azide **3** as a mixture of diastereomers (7:1 219 mg, 90% yield); *R*_f = 0.5 (hexanes/AcOEt 3:2, v/v); ¹H NMR (500 MHz, CDCl₃): δ = 7.39–7.30 (m, 10H), 5.15–5.03 (m, 4H), 4.96 (brs, 1H, NH), 4.89 (m, 1H, NH), 4.20 (m, 1H), 3.86–3.72 (m, 2H), 3.66 (t, *J* = 8.9 Hz, 1H), 3.50–3.40 (m, 1H), 3.34–3.26 (m, 1H), 3.07 (dd, *J* = 12.4, 3.0 Hz,

1H), 2.37 (brs, 1H), 2.34 (t, *J* = 6.3 Hz, 1H), 2.06–1.92 (m, 2H), 1.94 (m, 1H), 1.83 (m, 1H), 1.72–1.51 (m, 11H), 1.35 ppm (m, 1H); ¹³C NMR (63 MHz, CDCl₃): δ = 156.0, 155.6, 136.3, 136.2, 128.6, 128.5, 128.3, 128.2, 128.1, 111.8, 84.9, 82.0, 81.0, 67.1, 66.8, 55.5, 54.4, 52.1, 51.8, 49.6, 36.4, 30.8, 29.2, 25.0, 23.7 ppm; IR (neat): $\tilde{\nu}$ = 3309, 3032, 2931, 2096, 1699, 1523, 1230, 1042 cm⁻¹; HRMS-ESI: *m/z* calcd for C₂₈H₃₂N₂NaO₇: 531.2107 [*M*+Na]⁺; found: 531.2103.

Indicative click-chemistry protocol for the preparation of (2S,5S,6R,7S,8R,10S)-8,10-diamino-2-[(4-(hydroxymethyl)-1H-1,2,3-triazol-1-yl)methyl]-1-oxaspiro[4.5]decane-6,7-diol (13**):** The azide **4** (13 mg, 0.025 mmol) and propargyl alcohol (10 μL, 0.17 mmol) were dissolved in EtOH/H₂O (2:1, 2 mL) at room temperature. CuSO₄·5H₂O (2.0 mg, 8.0 × 10⁻³ mmol) was added to this solution, followed by sodium ascorbate (4.0 mg, 0.031 mmol), and the suspension was vigorously stirred for 18 h. The solvents were removed in vacuo and the crude product was directly purified by flash column chromatography on silica gel, with a CH₂Cl₂/MeOH (2:1) gradient elution system to afford the corresponding triazole. This was directly dissolved in water, KOH (0.18 g, 3.2 mmol) was added, and the mixture was warmed at 130 °C in a sealed tube. The solvent was removed in vacuo and the crude product was directly purified by flash column chromatography on silica gel, with a methanol to methanol/NH₄OH (aq.) (8:2) gradient elution system to afford the triazole **13** (4.7 mg, 60% yield over two steps). *R*_f = 0.2 (MeOH/NH₄OH (aq.) 9:1, v/v); ¹H NMR (500 MHz, D₂O): δ = 8.08 (s, 1H), 4.60 (m, 2H), 4.50 (m, 1H), 3.47 (t, *J* = 9.8 Hz, 1H), 3.42 (m, 1H), 3.00 (m, 1H), 2.89 (m, 1H), 2.23–2.08 (m, 3H), 1.97 (m, 1H), 1.86 (m, 1H), 1.53 ppm (q, *J* = 12.4 Hz, 1H); ¹³C NMR (63 MHz, D₂O): δ = 148.2, 126.6, 91.1, 81.8, 77.7, 77.5, 56.2, 55.6, 53.7, 52.2, 37.8, 31.8, 30.6 ppm; HRMS-ESI: *m/z* calcd for C₁₃H₂₄N₅O₄: 314.1828 [*M*+H]⁺; found: 314.1822.

Indicative fluorescence binding assay: Desalted and gel-purified RNA complementary strand oligonucleotides (Dharmacon, Inc.) were annealed in sodium cacodylate buffer (30 mM, pH 6.8) at 65 °C for 3 min, followed by snap cooling on ice. Hybridization was confirmed by analytical gel electrophoresis. The double-stranded construct contains the bacterial decoding site sequence in which the adenine at position 1492 has been substituted with the 2AP fluorescent analogue.

Titration of the tested compounds with the 2AP-labelled RNA bipartite construct were performed, with concentrations ranging from 10 pM to 1 mM. Emission spectra were recorded at RNA concentrations of 20 nM, 100 nM, 500 nM and 1 μM (30 mM sodium cacodylate, pH 6.8) in 1 cm pathlength quartz cells. Fluorescence was measured with a QuantaMaster 40 Steady State Spectrofluorimeter at 25 °C. The excitation wavelength used was 310 nm, whereas emission was monitored between 320 and 450 nm and normalized at maximum emission wavelength of 370 nm. Half-maximal response concentration (EC₅₀) values were calculated by fitting dose-response curves to the fluorescence intensities plotted against the logs of ligand concentrations. Three replicate experiments per compound were run. As control experiments, all ligands tested were also added to the 2AP-labelled single-stranded B oligonucleotide. Additionally, spermidine, a known nonspecific RNA binder, was titrated in parallel, as a negative dose-response control.

Acknowledgements

This research is supported by Marie Curie Actions, Excellence Teams (EXT) Grants, contract number MEXT-CT-2006-039149. We would also like to thank Dr. I. Mavridis for crystallographic support, Prof. E. Theodorakis for assistance with HR-mass spectroscopy.

py and Dr. S. Stratikos for assistance with the QuantaMaster 40 Steady State Spectrofluorimeter.

Keywords: aminoglycosides · click chemistry · ribosomal A site · rigid scaffolds · RNA recognition

- [1] J. R. Thomas, P. J. Hergenrother, *Chem. Rev.* **2008**, *108*, 1171–1224.
- [2] Q. Vicens, E. Westhof, *ChemBioChem* **2003**, *4*, 1018–1023.
- [3] T. Vacas, F. Corzana, G. Jiménez-Osés, C. González, *J. Am. Chem. Soc.* **2010**, *132*, 12074–12090.
- [4] Y. Tor, T. Hermann, E. Westhof, *Chem. Biol.* **1998**, *5*, R277–R283.
- [5] K. F. Blount, F. Zhao, T. Hermann, Y. Tor, *J. Am. Chem. Soc.* **2005**, *127*, 9818–9829.
- [6] J. L. Houghton, K. D. Green, W. Chen, S. Garneau-Tsodikova, *ChemBioChem* **2010**, *11*, 880–902.
- [7] a) I. A. Katsoulis, C. Pyrkotis, A. Papakyriakou, G. Kythreoti, A. L. Zografos, I. Mavridis, V. R. Nahmias, P. Anastasopoulou, D. Vourloumis, *ChemBioChem* **2009**, *10*, 1969–1972; b) T. Cottin, C. Pyrkotis, C. I. Stathakis, I. Mavridis, I. A. Katsoulis, P. Anastasopoulou, G. Kythreoti, A. L. Zografos, V. R. Nahmias, A. Papakyriakou, D. Vourloumis, *ChemBioChem* **2011**, *12*, 71–87.
- [8] C. I. Stathakis, I. Mavridis, G. Kythreoti, A. Papakyriakou, I. A. Katsoulis, T. Cottin, P. Anastasopoulou, D. Vourloumis, *Bioorg. Med. Chem. Lett.* **2010**, *20*, 7488–7492.
- [9] a) H. C. Kolb, M. G. Finn, K. B. Sharpless, *Angew. Chem.* **2001**, *113*, 2056–2075; *Angew. Chem. Int. Ed.* **2001**, *40*, 2004–2021; b) V. V. Rostovtsev, L. G. Green, V. V. Fokin, K. B. Sharpless, *Angew. Chem.* **2002**, *114*, 2708–2711; *Angew. Chem. Int. Ed.* **2002**, *41*, 2596–2599; c) M. Meldal, C. W. Tornøe, *Chem. Rev.* **2008**, *108*, 2952–3015.
- [10] A. Padwa, W. H. Pearson in *Synthetic Applications of 1,3-Dipolar Cycloaddition Chemistry Toward Heterocycles and Natural Products*, Wiley, New Jersey, **2003**.
- [11] N. K. Andersen, N. Chandak, L. Brulicová, P. Kumar, M. D. Jensen, F. Jensen, P. K. Sharma, P. Nielsen, *Bioorg. Med. Chem.* **2010**, *18*, 4702–4710.
- [12] C. Nájera, J. M. Sansano, *Org. Biomol. Chem.* **2009**, *7*, 4567–4581.
- [13] T. Takemoto, Y. Iio, T. Nishi, *Tetrahedron Lett.* **2000**, *41*, 1785–1788.
- [14] Y. Tamaru, M. Hojo, S. Kawamura, S. Sawada, Z. Yoshida, *J. Org. Chem.* **1987**, *52*, 4062–4072.
- [15] E. Rozners, Y. Liu, *Org. Lett.* **2003**, *5*, 181–184.
- [16] S. Shandrick, Q. Zhao, Q. Han, B. K. Ayida, M. Takahashi, G. C. Winters, K. B. Simonsen, D. Vourloumis, T. Hermann, *Angew. Chem.* **2004**, *116*, 3239–3244; *Angew. Chem. Int. Ed.* **2004**, *43*, 3177–3182.
- [17] W. Humphrey, A. Dalke, K. Schulten, *J. Mol. Graph.* **1996**, *14*, 33–38.
- [18] M.-P. Mingeot-LeClercq, P. M. Tulkens, *Antimicrob. Agents Chemother.* **1999**, *43*, 1003–1012.
- [19] Preliminary results relating to the biological activities of the compounds as functional bacterial translation inhibitors (coupled in vitro transcription-translation assay, IVT)^[7] revealed inconsistencies between binding affinities and interference of the synthetic compounds with the processes of protein production. Optimization of the assay conditions and further biological studies are currently underway.
- [20] M. B. Feldman, D. S. Terry, R. B. Altman, S. C. Blanchard, *Nat. Chem. Biol.* **2010**, *6*, 54–62.

Received: February 1, 2011

Published online on May 6, 2011